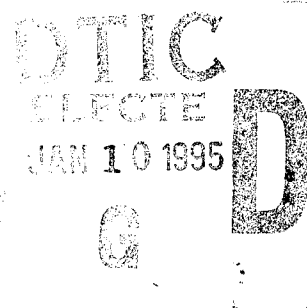# Addressing Tension Instability in SPH Methods

C.T. Dyka

Geo-Centers, Inc.
Fort Washington, MD

R.P. Ingel

Composites and Ceramics Branch
Materials Sciences and Technology Division

December 30, 1994

19950106 077

REPORT DOCUMENTATION PAGE

Public reporting burden for this collection of information is estimated to average 1 hour per response, including the time for reviewing instructions, searching existing data sources, gathering and maintaining the data needed, and completing and reviewing the collection of information. Send comments regarding this burden estimate or any other aspect of this collection of information, including suggestions for reducing this burden, to Washington Headquarters Services, Directorate for Information Operations and Reports, 1215 Jefferson Davis Highway, Suite 1204, Arlington, VA 22202-4302, and to the Office of Management and Budget. Paperwork Reduction Project (0704-0188), Washington, DC 20503.

1. AGENCY USE ONLY (Leave Blank)	2. REPORT DATE December 30, 1994	3. REPORT TYPE AND DATES COVERED Interim

4. TITLE AND SUBTITLE

Addressing Tension Instability in SPH Methods

5. FUNDING NUMBERS

6. AUTHOR(S)

C.T. Dyka* and R.P. Ingel

7. PERFORMING ORGANIZATION NAME(S) AND ADDRESS(ES)

Geo-Centers, Inc.   Naval Research Laboratory
10903 Indian Head Highway   Washington, DC 20375-5320
Fort Washington, MD 20744

8. PERFORMING ORGANIZATION REPORT NUMBER

NRL/MR/6384--94-7641

9. SPONSORING/MONITORING AGENCY NAME(S) AND ADDRESS(ES)

ARPA
Arlington, VA 22209

10. SPONSORING/MONITORING AGENCY REPORT NUMBER

11. SUPPLEMENTARY NOTES

*Geo-Centers, Inc., 10903 Indian Head Highway, Fort Washington, MD 20744

12a. DISTRIBUTION/AVAILABILITY STATEMENT

Approved for public release; distribution unlimited.

12b. DISTRIBUTION CODE

13. ABSTRACT (Maximum 200 words)

Smoothed particle hydrodynamics (SPH) has the potential to be an important method for structural analysis. However, the SPH method is currently plagued by tension instability. In this work, a new unconventional approach is introduced, in which the stresses are calculated at points other than the SPH nodes, to address this difficulty. This algorithm is implemented into a one dimensional (1D) program called SPH1D. In addition, objective stress rate calculations are discussed and specialized to 1D applications. The results from applying the unconventional approach to a simple bar are very encouraging. The bar holds together in tension and compares quite well to a finite element analysis.

14. SUBJECT TERMS		15. NUMBER OF PAGES
Explicit analysis SPH Fracture Transient Impact Wave propagation		23
		16. PRICE CODE

17. SECURITY CLASSIFICATION OF REPORT	18. SECURITY CLASSIFICATION OF THIS PAGE	19. SECURITY CLASSIFICATION OF ABSTRACT	20. LIMITATION OF ABSTRACT
UNCLASSIFIED	UNCLASSIFIED	UNCLASSIFIED	UL

CONTENTS

Accesion For		
NTIS CRA&I		☒
DTIC TAB		☐
Unannounced		☐
Justification		
By		
Distribution /		
Availability Codes		
Dist	Avail and / or Special	
A-1		

ADDRESSING TENSION INSTABILITY IN SPH METHODS

1. INTRODUCTION

Smoothed particle hydrodynamics (SPH) is a Lagrangian method that requires no spatial mesh. SPD is really an interpolation method in which particles can be employed as part of the approximation [1]. (Note that in this paper, the words element and particle will be used interchangeably when referring to SPH methods). The calculation of interactions among the particles is based upon their separation alone. This aspect along with the absence of a grid allows very large deformations to be computed in a straightforward fashion. In addition, arbitrary fracture surfaces can be opened without requiring special considerations such as an a priori knowledge of the fracture location as in finite element methods (FEM). SPH is thus an appealing and valuable computational tool, especially for high deformation events such as impact.

However, SPH is a maturing method and still has a few technical barriers to overcome before becoming a widely used tool in computational mechanics. Its biggest drawback is the well know instability in tension - premature fragmentation of the SPH grid in tension. Swegle et al. [2] have done a formal stability analysis that clearly discusses the roots of tension instability. Hicks et al. [3] have applied a conservative smoothing approach with some success, but tension instability remains a serious obstacle in general. Other difficulties with SPH methods include the accurate calculation of finite strains, inhomogeneous media, stress oscillations or "sawtooth" behavior (see [4]), and the application of natural boundary conditions.

In this paper, we present a new unconventional (UC) approach to address tension instability (and also oscillatory stresses) in which the stresses are calculated at points other than the SPH nodes. In addition, stress rate calculations are briefly addressed and specialized to one dimension (1D) applications.

1

2. THE SPH METHOD

The SPH method is non-local in nature and based upon interpolation - see [1], [4-6]. Consider the function $f(\underline{x})$ and its kernel average $\langle f(\underline{x}) \rangle$ expressed as:

$$\langle f(\underline{x}) \rangle = \int f(\underline{x}') \, W(\underline{x} - \underline{x}', h) dV' \qquad (1)$$

where V is the volume, $\underline{x}$ is the current position vector, and W is the kernel with a width measured by the parameter h. Various possibilities exist for the choice of $W(\underline{x} - \underline{x}', h)$ with the most popular being the cubic-b-spline [4]. The kernel W should satisfy the following condition:

$$lim_{h \to 0} \; W(\underline{x} - \underline{x}', h) = \delta(\underline{x} - \underline{x}') \qquad (2)$$

where δ is Dirac's delta function. Normalization of W and compact support (W is zero outside a limited domain) are expressed as:

$$\int W(\underline{x}, h) dV = 1 \qquad (3a)$$

and

$$W(\underline{x}, h) = 0 \qquad (|\underline{x}| > 2h) \qquad (3b)$$

Associating with a particle j, a volume

$$dV^j = \frac{M^j}{\rho^j} \qquad (4)$$

introduces the concept of particle mass, M^j, and density, ρ^j. The integral in (1) can then be replaced by the approximation:

$$\langle f(\underline{x}) \rangle \approx \sum_{j=1}^{N} f(\underline{x}^j) \, W(\underline{x} - \underline{x}^j, h) \, \frac{M^j}{\rho^j} \qquad (5)$$

where N is the total number of particles.

Dropping the $\langle \; \rangle$ sign, gradients of $f(\underline{x})$ can be expressed as [4]:

$$\nabla \left(f(\underline{x}) \right) = -\sum_{j=1}^{N} \frac{M^j}{\rho^j} f(\underline{x}^j) \frac{\partial W}{\partial x_l^j} e_l^j \qquad (6)$$

in which the subscripts denote component and e_l^j is the l component of the unit vector at j. Another form for the gradient of $f(\underline{x})$ that is widely used but which introduces additional approximation is [4]:

$$\nabla \left(f(\underline{x}) \right) = -\rho(x) \sum_{j=1}^{N} M^j \left[\frac{f(\underline{x})}{\rho^2(\underline{x})} + \frac{f(\underline{x}^j)}{\rho^2(\underline{x}^j)} \right] \frac{\partial W}{\partial x_l^j} e_l^j \qquad (7)$$

3. THE SPH EQUATIONS (BRIEFLY)

In subscript notation, the conservation of linear momentun is expressed as:

$$\frac{dV_m}{dt} = -\frac{1}{\rho} \frac{\partial \sigma_{mn}}{\partial x_n} \qquad (8)$$

in which V_m is the velocity and σ_{mn} is the Cauchy stress tensor, and the summation convention is implied by the repeated index n. Applying (6), (8) becomes at particle i:

$$\frac{dV_m^i}{dt} = -\frac{1}{\rho^i} \sum_{j=1}^{N} \frac{M^j}{\rho^i} \frac{\sigma_{mn}^j}{\rho^j} \frac{\partial W^{ij}}{\partial x_n^j} \qquad (9)$$

This form does not conserve momentum since the force on particle i due to j is not the same as j due to i. A widely used alternative to (9) that conserves momentum but introduces further approximation is obtained by substituting (7) into (8) to produce (no summation on i):

$$\frac{dV_m^i}{dt} = -\sum_{j=1}^{N} M^j \left[\frac{\sigma_{mn}^j}{(\rho^j)^2} + \frac{\sigma_{mn}^i}{(\rho^i)^2} \right] \frac{\partial W^{ij}}{\partial x_n^j} \qquad (10)$$

Artifical viscosity is usually included in the linear momentun as an artifical viscous pressure. Benz[1], Libersky and Petschek [2] and Libersky *et al.* [7] give details for including it into (10).

Mass conservation is of the form:

$$\frac{d\rho}{dt} = -\rho \frac{\partial V_m}{\partial x_m} \tag{11}$$

Introducing (7) into (11) produces:

$$\frac{d\rho^i}{dt} = -\rho^i \sum_{j=1}^{N} \frac{M^j}{\rho^j} V_m^j \frac{\partial W^{ij}}{\partial x_m^j} \tag{12}$$

A widely used alternative to (12) is [4]:

$$\frac{d\rho^i}{dt} = -\rho^i \sum_{j=1}^{N} \frac{M^j}{\rho^j} (V_m^i - V_m^j) \frac{\partial W^{ij}}{\partial x_m^j} \tag{13}$$

The density can also be directly determined from (5) and is of the form:

$$\rho^i = \sum_{j=1}^{N} M^j W^{ij} \tag{14}$$

Equation (14) will be employed in this paper.

In addition to momentum and mass conservation, energy conservation can also be included in the governing equations (see [1] and [2] for instance). In this work, it has not been introduced since a linear elastic material will be assumed.

4. CONSTITUTIVE EQUATIONS AND STRESS RATES

The current position $\underset{\sim}{x}(t)$ of the material point $\underset{\sim}{\bar{x}}$ can be expressed as:

$$\underset{\sim}{x}(t) = \underset{\sim}{\bar{x}} + \underset{\sim}{U}(t) \tag{15}$$

where $\underset{\sim}{U}(t)$ is the current displacement as measured from $\underset{\sim}{\bar{x}}$. In index notation, the rate of deformation $d_{mn}(t)$ is of the form:

$$d_{mn}(t) = \frac{1}{2}\left(\frac{\partial V_m}{\partial x_n} + \frac{\partial V_n}{\partial x_m}\right) \tag{16}$$

Note in (16), that d_{mn} is an Eulerian variable and the derivatives are with respect to x_n (not $\bar{x}_n$). The rate of deformation can be put in SPH form by directly applying either equation (6) or (7). In [2], further manipulations and approximations are introduced to produce the correct trace and to express $\underset{\sim}{d}$ in terms of velocity differences. For 1D applications, the use of (6) or (7) will suffice.

Next consider the velocity gradient L_{mn} which is defined by:

$$L_{mn}(t) = \frac{\partial V_m}{\partial x_n} \tag{17}$$

Using (16), L_{mn} can be divided into symmetric and skew-symmetric parts:

$$L_{mn} = d_{mn} + \theta_{mn} \tag{18}$$

where θ_{mn} is the rotation and given by

$$\theta_{mn} = \frac{1}{2}\left(\frac{\partial V_m}{\partial x_n} - \frac{\partial V_n}{\partial x_m}\right) \tag{19}$$

and d_{mn} is determined from (16).

Having defined the rate of deformation, we next seek an objective stress rate. The Jauman stress rate $\dot{\sigma}_{mn}^{jau}$ is widely used [8], and is expressed as:

5

$$\dot{\sigma}_{mn}^{jau} = \dot{\sigma}_{mn} - \theta_{lj}\sigma_{ml} - \theta_{lm}\sigma_{nl} \qquad (20)$$

where σ_{ml} and $\dot{\sigma}_{mn}$ are components of the Cauchy stress and the rate of Cauchy stress (which is not objective). For 1D applications, $\theta_{mn} = 0$ and

$$\dot{\sigma}_{11}^{jau} = \dot{\sigma}_{11} \qquad (21)$$

The Jauman stress rate can be related to the rate of deformation via the constitutive tensor $\underset{\sim}{C}$. In component form this relation is:

$$\dot{\sigma}_{mn} = C_{mnlq}d_{lq} \qquad (22)$$

For 1D applications and a linear material, (22) reduces to:

$$\dot{\sigma}_{11} = C_{1111}d_{11} \qquad (23)$$

where $C_{1111} = E$ (the modulus of elasticity and assumed to be constant), and

$$d_{11} = \frac{\partial V_1}{\partial x_1} \qquad (24)$$

Explicit integration of $\dot{\sigma}_{11}$ to obtain $\sigma_{11}(t)$ is in the form:

$$\sigma_{11}(t) = \sigma_{11}(t-dt) + \dot{\sigma}_{11}(t-dt)\,dt \qquad (25)$$

where dt is the current time step and from (23)

$$\dot{\sigma}_{11}(t-dt) = E \cdot d_{11}(t-dt)\,dt \qquad (26)$$

Because the displacement U_1 is the time derivative of V_1 and E is constant, (26) can be directly integrated in time to yield:

$$\sigma_{11} = E\bar{\varepsilon}_{11} \qquad (27)$$

where through (24)

6

$$\bar{\varepsilon}_{11}(t) = \frac{\partial}{\partial x_1} U_1(t) \tag{28}$$

Equations (6) or (7) are then introduced into (28) to express $\bar{\varepsilon}_{11}(t)$ in a SPH form. We note that $\bar{\varepsilon}_{11}$, which is determined by integrating d_{11} in time, is not the well known linear strain. Rather it is an Eulerian variable because the derivative in (28) is with respect to $x_1(t)$ not $\bar{x}_1$.

5. ADDRESSING TENSION INSTABILITY

Tension instability is a problem that has longed troubled conventional SPH methods and greatly limited its application. In [2], a stabiltiy analysis for 1D is presented. That analysis shows SPH calculations to be unstable when:

$$\left(\frac{\partial^2 W}{\partial x^2}\right)\sigma_{11} > 0 \tag{29}$$

This means that the standard SPH method, in which the node and the stress point are both located at the centroid of the element (particle), will be unstable in tension. Swegle *et al.* in [2] also demonstrate that this tension instability can not be corrected by artifical viscosity.

The approach in this work to overcome tension instability is indicated in Fig. 1, in which the stress points (denoted by x) are computed at points away from the SPH nodes (denoted by o and located at the center) as measured by the distance R. The limits of R are:

$$0 \le R \le 0.5 \tag{30}$$

$R = 0.5$ corresponds to the conventional form in which both stress points are located at the centroid of the element, while $R = 0$ places the two stress points at the left and right edges of the element. In conventional SPH because the stress points coincide with the SPH node, particle i does not enter into the calculation of σ^i_{11}, since

7

$\dfrac{\partial W^{ij}}{\partial x^j} = 0$ for a symmetric kernel when $i = j$. In this new approach, which we refer to as unconventional or UC, for $0 \leq R < 0.5$ node i will be included in the stress calculations for SPH element i. Thus stress calculations from the unconventional approach should be more accurate since node i will be included at the stress points i_a and i_b (see Figure 1). Also the UC method should help to lessen or eliminate oscillation or the "sawtooth" effect evident in standard SPH stress calculations [4].

In additon and more importantly, however, the UC approach should also help to address the tension instability present in the conventional ($R = 0.5$) SPH. The reason for this is as follows. Assume a uniform 1D grid, as shown in Fig. 1, with the smoothing length $2h = 2L$, where L is the length of each SPH element. For the conventional approach, all nodes for the SPH gradient calculations are at least h (=L) distance away, and node i is not included in any of the calculations for stress and linear momentum at i. In [2], it has been shown that instability in tension is governed by (29), and for the standard cubic-b-spline kernel this is satisfied in tension whenever $x_{ij} > 0.6h$ (approximately). Unfortunately for conventional SPH methods, (29) is satisfied for all the SPH nodes included in the gradient calculations at node i. As mentioned above for the UC approach, node i is included in the stress calculations at the stress points i_a and i_b ($R < 0.5$) as shown in Fig. 1. Also, the stress points i_a and i_b will be included in the linear momentum calculated at node i. Thus, (29) will not be satisfied at these two stress points. In addition, the two SPH elements adjacent to i, $i - 1$ and $i + 1$, may also contain stress points (depending on the value of R) which do not satisfy (29). Therefore, the UC method should have a strong stabilizing effect on the SPH mesh in tension, not allowing it to prematurely fragment.

8

6. NUMERICAL IMPLEMENTATION - SPH1D

For the unconventional (UC) formulation in our 1D code SPH1D, four options have been programmed for the calculation of stress and linear momentum. These options are specified by the parameter JSP. Gradient calculations used to determine the stress (σ_{11}) employ either (6) or (7) in this work. Linear momentum calculations are based on either (9) or (10). Recall that (9) does not conserve momentum, but for the UC formulation (6) and (9) are more accurate than (7) and (10). Equations (7) and (10) represent the standard SPH approach in which additional approximations have been introduced [4,5].

JSP = 1 corresponds to the use of (7) and (10) or the standard SPH particle equations, but with the UC formulation in which the stress points are not located at the SPH nodes ($0 \leq R < 0.5$). For JSP = 2, (6) is employed for the stresses while (9) is used for linear momentum calculations. JSP = 3 uses (6) for the stresses and (10) for linear momentum. Thus, options JSP =1 and 3 introduce additional approximations for the UC, but (10) does enforce the conservation of momentum. Also it is noted that for the linear momentum calculations using either (9) (JSP =2) or (10) (JSP = 1 or 3), each of the two stress points within a particular SPH element (particle) is assumed to possess one half of the total mass of that element - this allows retention of the particle concept. In addition, when using (10) (JSP = 1 or 3), the stress at the typical SPH node i, since it is not calculated, is assumed to simply be the average of the two stress points i_a and i_b (see Fig. 1) in that element.

The fourth option (JSP = 4) in SPH1D uses the same equations as JSP =2 , or (6) for stress calculations and (9) for linear momentum. However, with JSP = 4 the stress σ_{11} is calculated through (6) and (27) and (28) only at the element centroid (as if $R = 0.5$ in Figure 1) and it is assumed that:

$$\sigma_{11}^{i} = \sigma_{11}^{i_a} = \sigma_{11}^{i_b} \tag{31}$$

So σ_{11} is assumed to be constant in SPH element i. Linear momentum is then calculated using (9) but with the stresses applied not at i (the centroid) but rather at i_a and i_b as specified in the UC approach when $0 \le R < 0.5$. The option JSP = 4, thus represents a compromise between the conventional and unconventional SPH approaches, that may at least help to stabilize the mesh in tension, although not addressing stress oscillation or "sawtooth" behavior.

Ghost particles are employed for the application of essential boundary conditions. See [5] for the enforcement of free and fixed end conditions. Also, explicit time integration in the form of a modified central difference (MCD) method is applied to the linear momentum equations. Taylor and Flanagan [9] briefly discuss the MCD method which consists of a forward difference to compute the velocities followed by a backward difference to calculate the displacements. In equation form the MCD is:

$$\underline{V}(t) = \underline{V}(t - dt) + dt \cdot \underline{A}(t - dt) \tag{32a}$$

$$\underline{U}(t) = \underline{U}(t - dt) + dt \cdot \underline{V}(t) \tag{32b}$$

where $\underline{A}$ is the acceleration and dt is the time increment.

Overall, the SPH1D program is a relatively simple 1D code, but it will be a useful platform to demonstrate our unconventional approach. Finally, in SPH1D only a linear elastic material model has been implemented at this point.

7. APPLICATION

In this section as test of our unconventional approach, the SPH1D code will be applied to the elastic 1D bar described in Fig. 2. The bar is fixed at the right end B and the left one quarter of the bar is given an initial velocity of V_0=-5 m/sec, thus putting the bar in tension initially. Standard SPH methods $(R = 0.5)$ can not solve this problem due to the tension instability that will immediately develop. As indicated in Fig. 2a, the SPH grid is very coarse with only 40 uniform SPH elements (particles) used in the model. A comparable finite element model using the ABAQUS [10,11] program that consists of 40, 2D solid elements is described in Fig. 2b.

Fig. 3 presents the displacement time history of the left end A (SPH node 1 actually) for the UC results with $R = 0.25$ (so the stress points are at the quarter points of the SPH elements). Also included are the finite element method (FEM) results using ABAQUS with implicit time integration, which is unconditionally stable. The time step used for the explicit SPH calculations as well as for the implicit FEM model is dt = 0.4 E-6 sec. This time step is based upon an estimate of the Courant stability limit of approximately 0.66 E-6 sec., which is determined by dividing the length of the typical SPH element by the wave speed C.

As indicated in Fig. 3, the SPH1D results (solid line) with $R = 0.25$ are very close to the ABAQUS predictions (dashed line) for the displacement history at the left end of the bar, point A. Some slight phase difference between the two analyses develops later but this is probably due to the use of an explicit solver for SPH1D and an implicit solver for ABAQUS, as well as basic differences between the SPH and FEM forms of discretization.

The JSP = 2 option was used to generate Fig. 3. This option in SPH1D employs (6) for stress calculations and (9) for linear momentum. The use of the other options, JSP =1,3 which employ (10) and do conserve momentum as well as JSP = 4, produced results that eventually went unstable. JSP = 4 went unstable the quickest in the analysis. Reducing the timestep dt and increasing the artifical viscosity did not stabilize the SPH1D calculations for JSP =1, 3 or 4. Only JSP =2 remained stable and all the results in this section used that option.

Various values for R in the approximate range of $0 \leq R \leq 0.40$ produced SPH results very similar to Fig. 3 in which $R = 0.25$. For the range $0.4 < R \leq 0.5$, the response of the bar tended to be become unstable as the two stress points approached the centroid of the SPH element ($R = 0.5$).

Fig. 4 indicates the predicted time history for the velocity of the left end A for SPH1D and ABAQUS. In general, the agreement is excellent with again some slight phase differences developing as the analysis goes on.

11

In Figs. 5 and 6, the stress σ_{11} at SPH node 11 (stress point 11_a) is compared to σ_{11} at the centroid of finite element 11 - point C in Figs. 2a and 2b. Fig. 5 indicates the extended time history of σ_{11}. Fig. 6 plots the results only up to .0002 sec. so that the differences in the two analyses are more evident. As indicated in Fig. 6, early in the analysis especially the SPH1D stress results do tend to fluctuate more than the ABAQUS results . In general, the SPH1D predictions for σ_{11} compare reasonably well to ABAQUS, but not as well as did the displacement and velocity at A as indicated in Figures 3 and 4. This is not too surprising since stress is determined by differentiating the displacement, and the mesh is very coarse with only 40 SPH and 40 FEM elements used in the analyses.

The 1D bar is next given an initial velocity of $V_0 = 5$ m/sec, thus putting the bar in compression initally. This is done to determine the effect of the UC formulation on the stress oscillation or "sawtooth" behavior encountered in the standard or conventional SPH approach ($R = 0.5$). Putting the bar initially in compression allows a comparison between the UC and the conventional SPH, since the latter is not stable in tension. Fig. 7 shows a snapshot of the stress σ_{11} along the entire bar at t = 1.0 E-5 sec. The UC results with $R = 0.25$ are indicated by the solid line, and the conventional SPH results in which $R = 0.5$ are depicted by the dashed line. In general, we see that the UC results are much smoother indicating a lessening of the "sawtooth" behavior.

8. CONCLUSIONS

In this work, tension instability has been addressed for SPH methods. A new unconventional (UC) approach has been presented in which the stresses are computed at points away from the SPH nodes. The location of these two stress points within a 1D SPH element (particle) is controlled by the parameter R. The UC approach removed the tension instability in the bar considered for R in the approximate range of $0 \leq R < 0.45$. No optimum value of R was found in general. UC displacement and velocity results were in excellent agreement with a comparable ABAQUS finite ele-

12

ment model. Axial stress comparison to the ABAQUS model were not quite as good, but that probably is to be expected given the coarseness of the meshes and the non-local nature of the SPH method, which interpolates outside the SPH element (unlike FEM). In a comparison to standard SPH ($R = 0.5$) for the bar in compression initially, the UC seemed to alleviate the stress oscillation or "sawtooth" effect.

The UC approach was successful in removing tension instability, but only for the option JSP = 2, in which (6) and (9) were used for the stress and momentum calculations. Equations (6) and (9) are not widely used in the SPH literature, and (9) does not conserve momentum. These are important points to note with the UC approach.

Unfortunately, the JSP =4 option (like JSP =1 and 3) failed to remain stable for the UC method. If this option had been successful, modifications to existing SPH codes would have been easier and less expensive since only one stress point (the centroid) within each particle would have to be tracked.

Overall, based on the results from the simple 1Dbar, the use of the unconventional approach for SPH calculations is very encouraging. This approach can be extended to 2D and 3D problems, but this will be computationally expensive since additional stress points within each SPH element have to be tracked in the analysis besides just the centroid. Also, extension to 2D and 3D may require a rethinking of the overall particle concept. Finally, perhaps a method analogous to hourglass control for reduced integration in finite element techniques [11] may be possible with the UC method.

9. ACKNOWLEDGMENTS

10. REFERENCES

1. W. Benz, Smooth particle hydrodynamics: a review. *Numerical Modeling of Non-linear Stellar Pulsation: Problems and Prospects*, Kluwer Academic, Boston, (1990).

2. J. W. Swegle, D. L. Hicks, and S. W. Attaway, SPH stability analysis. *A Colloquium on Advances in Smooth Particle Hydrodynamics*, Albuquerque (1993).

3. D. L. Hicks, J. W. Swegle, and S W. Attaway, Smoothing and SPH. *A Colloquium on Advances in Smooth Particle Hydrodynamics*, Albuquerque (1993).

4. J. W. Swegle, S. W. Attaway, M. W. Heinstein, F. J. Mello, and D. L. Hicks, *An Analysis of Smoothed Particle Hydrodynamics*. Sandia National Lab, Report No. SAND93-2513UC-705, Albuquerque, March (1994).

5. L. D. Libersky and A. G. Petschek, Smooth particle hydrodynamics. *Proc., The Next Free Lagrange Conference, Jackson Hole, WY*, 1990 (Edited by H. E. Trease, J. W. Fritts, and W. P. Crowley), Springer-Verlag, New York (1991).

6. J. J. Monaghan, Smoothed particle hydrodynamics. *Annu. Rev. Astron. Astrophys.* **30**, 543-574 (1992).

7. L. D. Libersky, A. G. Petschek, T. C. Carney, J. R. Hipp and F. A. Allahdadi, High strain Lagrangian hydrodynamics: a three dimensional SPH code for dynamic material response. *J. Comput. Phys.* **109**, 67-75 (1993).

8. D. J. Benson, Computational methods in Lagrangian and Eulerian hydrocodes. *Comp. Meth. App. Mech. Engin.* **99**, 235-394 (1992).

9. L. M. Taylor and D. P. Flanagan, *PRONTO2D, A Two Dimensional Transient Solids Dynamics Program*. Sandia National Lab, Report No. SAND 86-0594UC-32, Albuquerque, March (1987).

10. *ABAQUS Theory Manual, Version 5.2*. Hibbitt, Karlsson and Sorensen, Inc., Pawtucket, RI (1992).

11. *ABAQUS User's Manual, Volumes 1 and 2, Version 5.2*. Hibbitt, Karlsson and

Sorensen, Inc., Pawtucket, RI (1992).

12. R. D. Cook, D. S. Malkus, and M. E. Plesha, *Concepts and Applications of Finite Element Analysis,* 3rd Edn. Wiley, New York (1989).
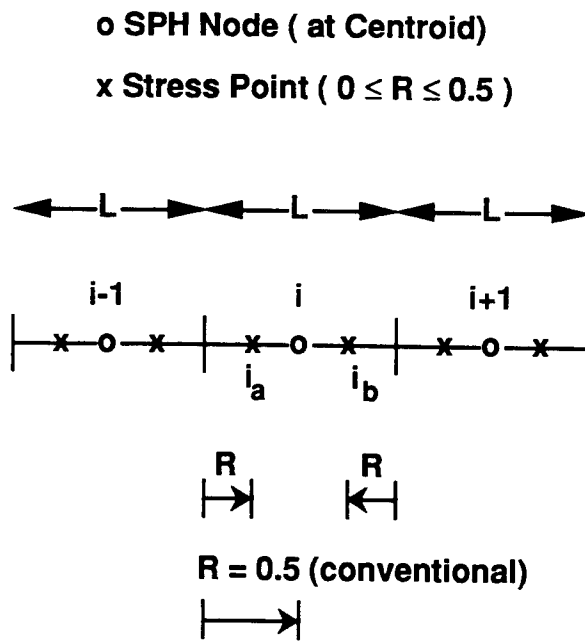
o SPH Node (at Centroid)

x Stress Point ($0 \leq R \leq 0.5$)

Figure 1. Typical 1D SPH elements for the unconventional approach. When $R = 0.5$ have the conventional SPH method.

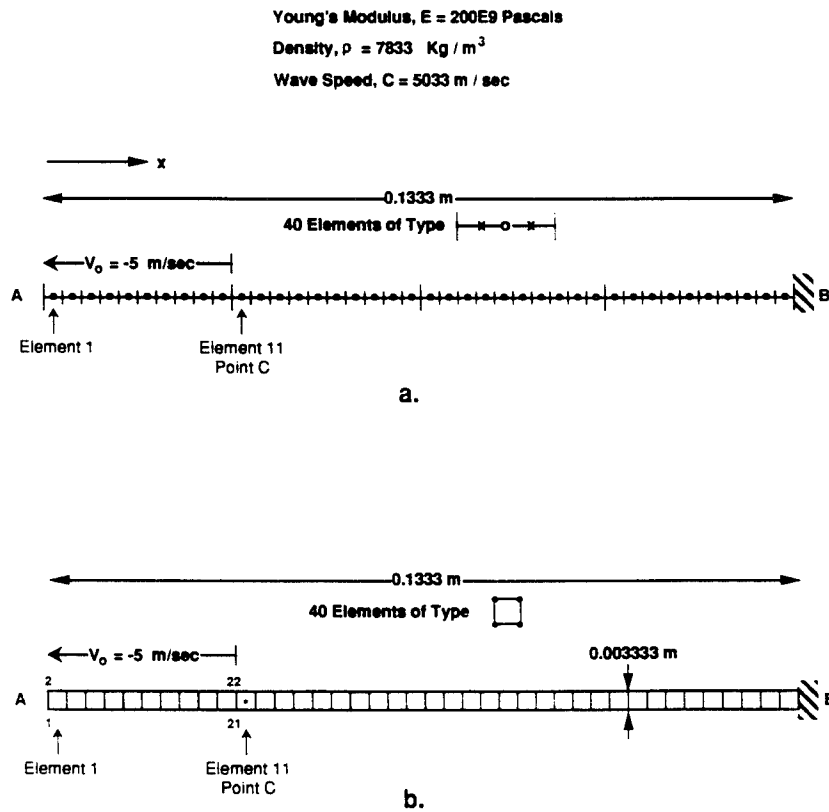Young's Modulus, E = 200E9 Pascals

Density, ρ = 7833 Kg / m^3

Wave Speed, C = 5033 m / sec

$\longrightarrow$ x

$\longleftarrow$ 0.1333 m $\longrightarrow$

40 Elements of Type $\vdash$—x—o—x—$\dashv$

$\longleftarrow V_o = -5$ m/sec $\longrightarrow$

A ... B

Element 1

Element 11
Point C

a.

$\longleftarrow$ 0.1333 m $\longrightarrow$

40 Elements of Type □

$\longleftarrow V_o = -5$ m/sec $\longrightarrow$

0.003333 m

2   22

A   B

1   21

Element 1

Element 11
Point C

b.

Figure 2. A simple bar given an initial velocity: (a) SPH1D grid, (b) ABAQUS FEM grid.

17
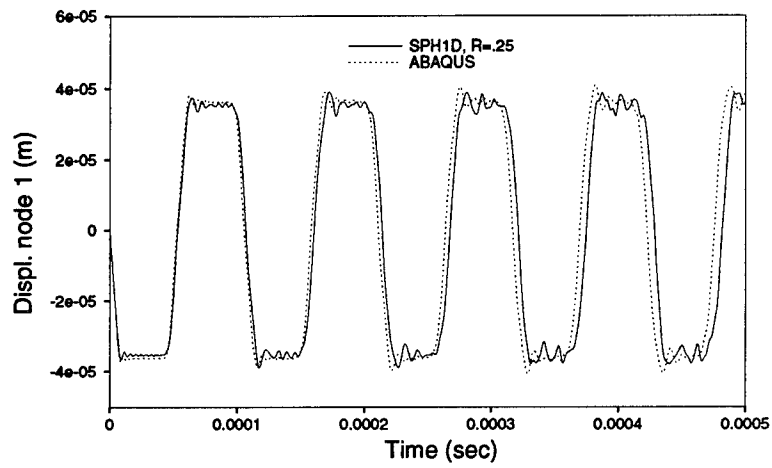
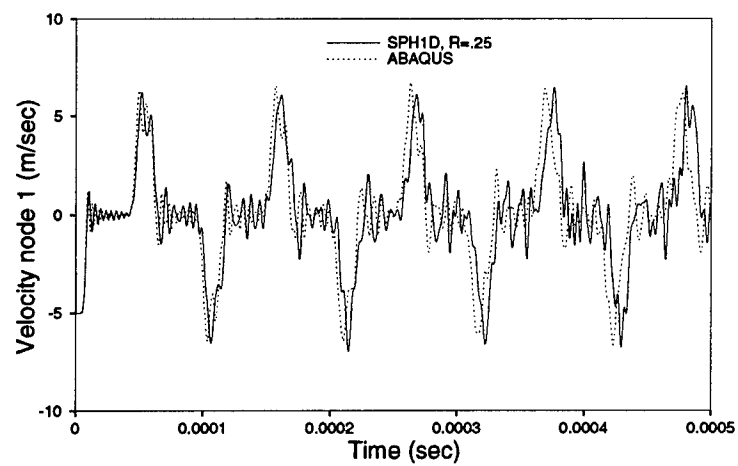Figure 3. Displacement history for the left end of the bar (point A).

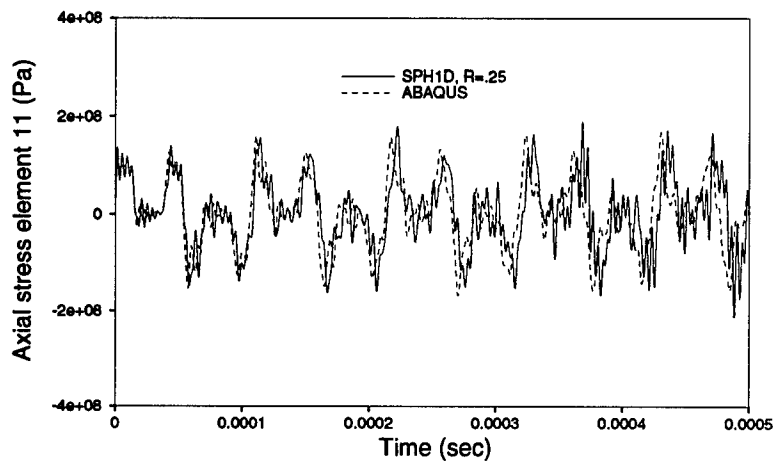Figure 4. Velocity history for the left end of the bar (point A).

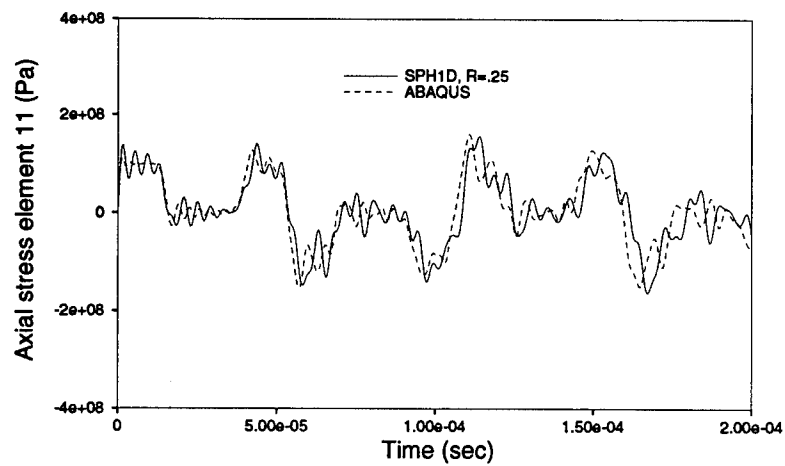Figure 5. Extended stress history at node 11 (point C).

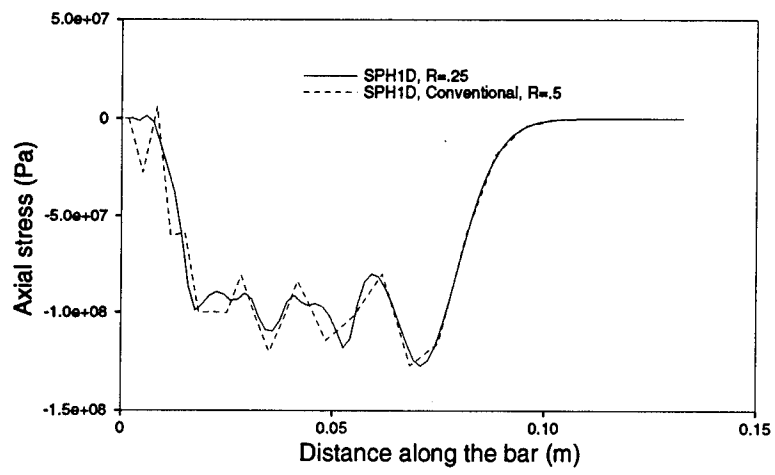Figure 6. Early stress history at node 11 (point C).

19

Figure 7. SPH1D UC and conventional stress predictions for the bar at t = 1.0E-5
sec (V_0 = .5 m/sec).